The Craze-Tip Deformation Zone in PC/SAN Microlayer Composites

K. SUNG, D. HADERSKI, A. HILTNER,* and E. BAER

Department of Macromolecular Science and Center for Applied Polymer Research, Case Western Reserve University, Cleveland, Ohio 44106

SYNOPSIS

Crazing in styrene-acrylonitrile copolymer (SAN) layers of polycarbonate (PC)/SAN microlayer composites and the deformation zone that formed in the PC layer in response to the stress concentration created at the PC/SAN interface by the craze tip were examined by optical and scanning electron microscopy. A 49-layer composite with relatively thick layers, on the size scale of tens of microns, was chosen in order to confine interactions to the region of a single PC/SAN interface. The SAN craze density, which increased with applied stress, was shown to fit the Weibull distribution function. The distance between crazes was described by a correlation length, and the distribution of correlation lengths indicated that crazing occurred randomly in the SAN layers. In the PC layer, the craze-tip deformation zone consisted of a colinear plastic zone together with a pair of micro-shearbands that grew away from the craze tip at an angle of about 45°. Assuming a blunted craze tip, the plastic zone was analyzed using the slip-line field theory. The dependence of the micro-shearband length on remote stress was similar to that predicted by both the BCS and Vitek models. © 1994 John Wiley & Sons, Inc.

INTRODUCTION

The microdeformation behavior of polycarbonate/styrene–acrylonitrile copolymer (PC/SAN) microlayer composites has been described.[1-3] For these studies, a series of microlayer composites was available with a variation in the individual layer thickness of PC and SAN of two orders of magnitude, from less than 1 micron to tens of microns. This range of layer thickness was achieved by varying the total number of layers, ranging from 49 to 1857, and by varying the volume ratio of the two components. The first observable irreversible deformation was always crazing in the SAN layers; subsequently, micro-shearbanding in the PC layers initiated at the craze tips. When the layers were thin enough, on the size scale of microns, interactive deformation phenomena were observed. Instead of random crazing of the SAN layers, craze doublets, which consisted of two aligned crazes in neighboring SAN layers, and craze arrays, with many aligned crazes in neighboring SAN layers, were observed.[3] In addition, interactive shear modes caused a change in the deformation mechanism of the SAN layers from crazing to micro-shearbanding close to the point of global yielding. This change in deformation mechanism of the SAN layers was responsible for increased ductility and toughness in composites with thinner layers.

To understand how the initial events of crazing and micro-shearbanding led to interactive phenomena, it was useful to first characterize the deformation zone that formed in the PC layer at the craze tip. Of the many PC/SAN microlayer composites in the series, the one with the thickest PC layers was chosen for this study in order to confine the deformation zone to the region of a single PC/SAN interface. This was a composite with 49 layers in which the PC layers were 29 μm thick and the SAN layers were 16 μm thick. Crazing in the SAN layers was described by a statistical analysis. Subsequent shear deformation in the PC was understood by considering the known shear yielding modes of PC.

* To whom correspondence should be addressed.

Journal of Applied Polymer Science, Vol. 52, 135–145 (1994)
 CCC 0021-8995/94/020135-11

MATERIALS AND METHODS

Microlayer composites of polycarbonate (PC) and styrene–acrylonitrile copolymer (SAN) were provided by The Dow Chemical Co. As described previously,[3] a series of compositions was available in which the individual layer thicknesses of PC and SAN were changed by varying the total number of layers, ranging from 49 to 1857, and by varying the volume ratio of the two components. Of the many composites in the series, the one with the thickest PC layers was chosen for this study. This composite consisted of 49 alternating layers with PC as the outermost layer; the thickness of the PC layers determined from optical micrographs was 29 μm and that of the SAN layers was 16 μm. In the format used previously, this composite was identified as 49-layer PC/SAN (29/16 μm).[3]

Microspecimens 0.8 mm thick were prepared by sectioning along the edge of the coextruded sheet with a low-speed diamond saw (Isomet, Buehler Ltd.). The cut surfaces of the specimen were polished on a metallurgical polishing wheel initially with 1200 and 2400 grit wet sandpapers and subsequently with 1.0 and 0.3 μm alumina aqueous suspensions. A thinner gauge section was prepared by polishing to a thickness of about 0.5 mm in order to confine the deformation to a central region of the specimen.

The polished specimen was clamped into a microtensile tester (Minimat, Polymer Laboratories) that was mounted on the stage of an optical microscope (Olympus BH2). Then, the specimen was stretched at a speed of 0.01 mm/min and the specimen was photographed as it was deformed. The strain was determined directly from the displacement; the local strain measured from craze positions was within 10% of the remote strain.

For scanning electron microscopy (SEM), specimens were first deformed in the Minimat to the desired strain and then reloaded to the same strain in a modified SEM stage. The restretched specimens were coated with 30 Å of gold and observed under load in a low-voltage scanning electron microscope (JEOL JSM-840A).

RESULTS AND DISCUSSION

Statistics of Crazing

A statistical approach was used to describe the gradual increase in craze density in the SAN layers when a PC/SAN microlayer composite was deformed in uniaxial tension. Data for statistical analysis were obtained by repeatedly photographing the same area of a microspecimen as it was subjected to increasing tensile deformation. The center region of the microspecimen where the layer thickness was the most uniform was used for this purpose. Once the craze initiation condition was achieved in the SAN layers, the overall craze density gradually increased until shear bands appeared in the PC layers at the craze tips. The cumulative craze fraction (F_c) was defined as the ratio of the number of crazes (N_c) in the area chosen to the total number of crazes (N_t) in the same area after neck formation. The total number of crazes (N_t) in a typical area analyzed was about 90.

The Weibull failure distribution is widely used in engineering practice due to its versatility. It takes its name from the Swedish research engineer W. Weibull who proposed it in 1949 for the interpretation of fatigue data. Since then, the application of this failure distribution has been extended to many other problems, particularly in the field of lifetime phenomena. In polymers, the statistics of craze fibril breakdown have been found experimentally to follow a Weibull distribution.[4]

The three parameter Weibull distribution for craze density with respect to the applied stress is given by[5]

$$F_c = \begin{cases} 0 & \sigma_{SAN} \leq \sigma_i \\ 1 - \exp\{-[(\sigma_{SAN} - \sigma_i)/\sigma_q]^m\} & \sigma_{SAN} > \sigma_i \end{cases} \quad (1)$$

where m is the Weibull "modulus" or shape parameter; σ_i, the location parameter; and σ_q, the scale parameter. The stress in the SAN layer, σ_{SAN}, was calculated according to the rule of mixtures for constant strain by the following equation:

$$\sigma_{SAN} = \sigma/[V_{SAN} + (E_{PC}/E_{SAN}) \cdot V_{PC}] \quad (2)$$

where V_{PC} and V_{SAN} are the volume fractions of PC and SAN in the composite, respectively, and E_{PC} = 2.32 GPa and E_{SAN} = 3.43 GPa are the elastic moduli for PC and SAN controls.

The Weibull plot of the cumulative craze fraction with respect to stress in the SAN layer for PC/SAN (29/16 μm) is shown in Figure 1. The Weibull location parameter σ_i accounts for the arbitrary origin of the random variable and corresponds to the craze initiation stress; σ_q is the characteristic stress, when $\sigma_{SAN} = \sigma_i + \sigma_q$, $F_c = (e - 1)/e$ or 63%; and m is the shape parameter that describes the width of the dis-

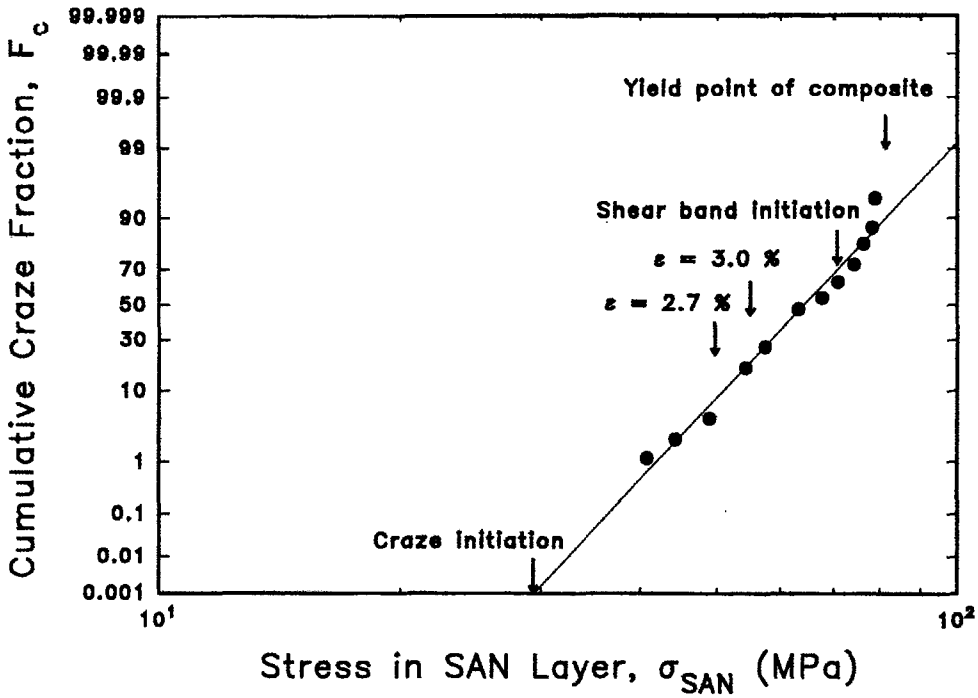

Figure 1 Weibull distribution plot of the cumulative craze fraction vs. the stress in the SAN layer.

tribution and is obtained from the slope of the Weibull plot. The best fit of the data was obtained with values of σ_i = 29.0 MPa, σ_q = 38.0 MPa, and m = 4.

Distribution of Crazes

The location of crazes in the SAN layers relative to one another was characterized by a correlation length R. Several consecutive photographs from the center region of the microspecimen where the layer thickness was the most uniform were used for this purpose. A reference line was chosen perpendicular to the layer orientation, and each craze was given a one-dimensional coordinate corresponding to the distance from the reference line. The correlation length (R) was defined as the perpendicular distance between two crazes; the length unit of R was defined as 1 μm. The definition of correlation length is illustrated in Figure 2.

With a short computer program, the distance between any two crazes was calculated for $R \leq 60$ and the absolute values were sorted according to whether they were correlation lengths between crazes in the same SAN layer, crazes in first-neighboring SAN layers, crazes in second-neighboring SAN layers, etc. In each of the sorted categories, the probability of a particular R value was then given by

$$Q(R) = N(R)/N_t \quad (3)$$

where $N(R)$ is the total number of correlation lengths having a value R, and N_t, the sum of all the $N(R)$'s for correlation lengths between 0 and 60.

The probabilities of R values between 0 and 20 are plotted in Figures 3 and 4 for two strains: 2.7% (F_c = 0.08) and 3.0% (F_c = 0.20). Since negative and positive R values were indistinguishable, the region close to R = 0 was emphasized by plotting $Q(R)$ vs. both $+R$ and $-R$. The figures include probabilities for crazes in the same layer and the first-, second-, and third-neighboring layers. If crazing occurred randomly, the probability would be 1/60 or 0.0167. This value is indicated by the solid line superimposed on the data in the figures. A higher value would indicate stress intensification and a lower value stress reduction. At both strains, the probability that the distance between two crazes in the same layer would be less than 5 μm was almost zero, and the probability that the distance would be between 5 and 10 μm was less than the random probability. This well-known effect was due to stress relief in the surrounding material after a craze formed.[6] The distribution of correlation lengths between crazes in neighboring SAN layers was constant and equal to the random distribution, indicating that crazes in one SAN layer had no effect on crazing in neighboring SAN layers.

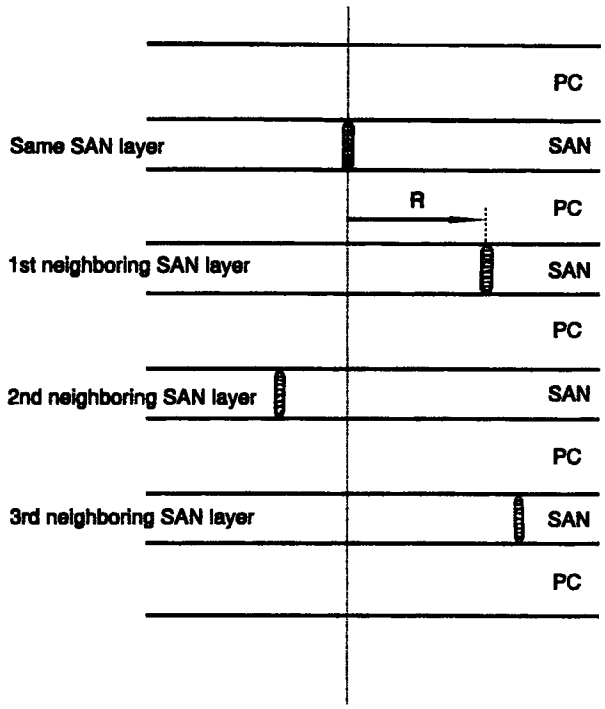

Figure 2 Definition of the correlation length between crazes.

Deformation Zone at the Craze Tip

A scanning electron micrograph of the craze tip in a specimen strained to about 5% revealed that the craze did not grow through the interface into the PC layer; instead, the craze tip was blunted at the layer interface (Fig. 5). Blunted crazes gradually opened as the strain increased, but did not penetrate through the interface into the PC layer. The relationship between craze opening and the remote strain in Figure 6 showed gradual opening of the crazes between 2.5% strain, about where crazing initiated, and 6% strain, close to the yield point. This meant that progressive widening of existing crazes occurred simultaneously with formation of new crazes. At higher strains, widening of the crazes was accompanied by fracture of craze fibrils at the surface.

A typical optical micrograph of crazes at 5.5% strain is shown in Figure 7. In addition to the pair of shear bands that originated at the craze tip, a dark line extended 1–2 μm from the tip of the craze into the adjacent PC layer. Since examination of the craze tip in the SEM did not reveal any evidence of a crack or craze growing into the PC layer from

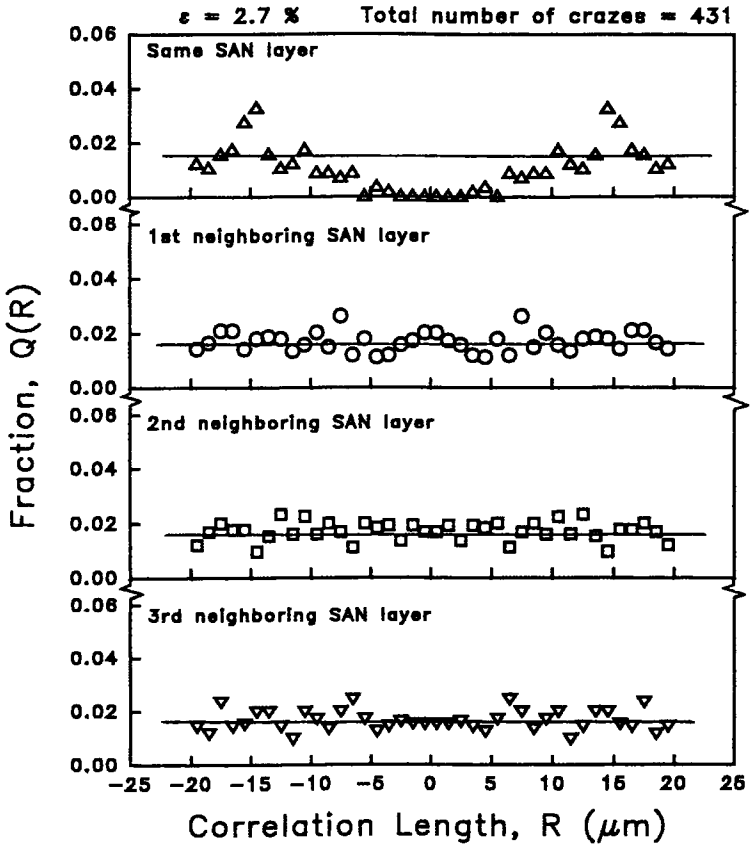

Figure 3 Distribution of correlation lengths in the same SAN layer and the first-, second-, and third-neighboring SAN layers at 2.7% strain.

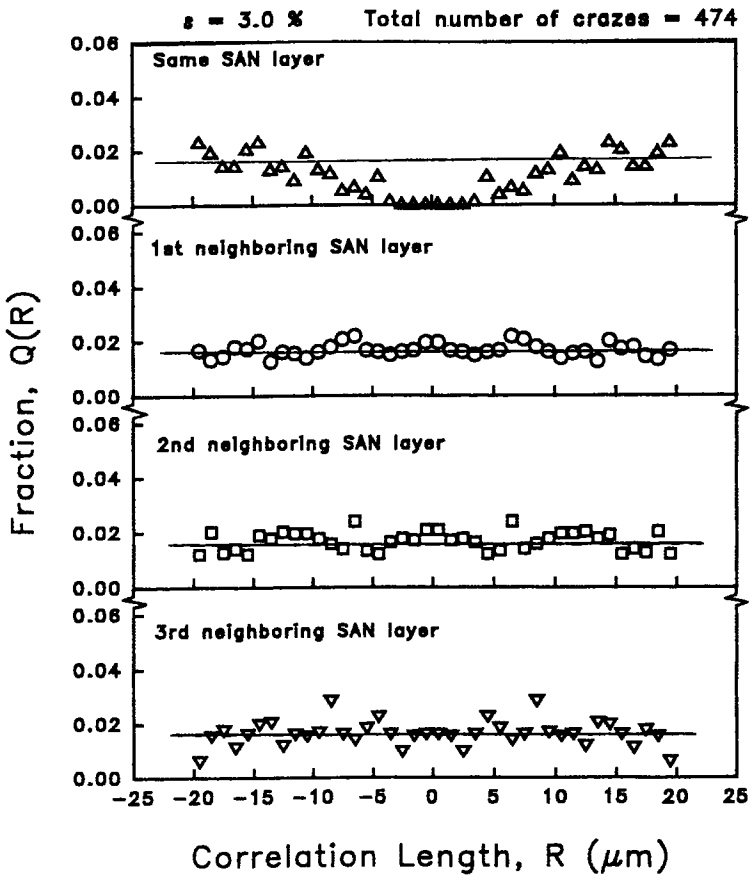

Figure 4 Distribution of correlation lengths in the same SAN layer and the first-, second-, and third-neighboring SAN layers at 3.0% strain.

the SAN craze tip, the dark line in the optical micrographs was attributed to light scattering from a small plastic zone that formed in the PC layer in response to the stress concentration created by the craze tip. Because the craze-tip plastic zone did not produce appreciable surface distortion, it was not visible in the SEM. The length of the craze-tip plastic zone (L_p) was measured from optical micrographs and the average of at least 10 measurements at each strain is plotted as a function of the remote strain in Figure 8. A craze-tip plastic zone was first detectable in the optical microscope at a strain of about 3%; the zone subsequently lengthened linearly with increasing strain.

The craze-tip plastic zone had grown to about 1.3 μm in length at 4.5% strain when micro-shearbands growing from the craze tip at an angle of about 45° could first be unambiguously identified in the optical micrographs. The micro-shearbands were clearly distinguishable from the craze-tip plastic zone only when they were about the same length as the plastic zone, 1.0–1.5 μm. The micro-shearband length is also included in Figure 8. Between 4.5% strain and the onset of global necking at about 6.2% strain, deformation in the PC layers was characterized by rapid growth of the micro-shearbands into the PC layer and by continued lengthening of the plastic zone as crazes in the SAN layers opened up further.

Formation and growth of the craze-tip plastic zone and the micro-shearbands in the PC layer at the tip of an SAN craze are summarized schematically in Figure 9. Formation of the crazes was easily detected in the optical microscope when the remote strain was about 2%. As the strain increased to about 3.5%, the craze density increased rapidly and the existing crazes widened. Adhesion between SAN and PC was good enough that the layers did not delaminate when the SAN craze impinged on the layer interface. Instead, the opening crazes were blunted at the layer interface, and a small colinear plastic zone formed in the PC layer in response to the stress concentration created by the blunted craze tip. The craze-tip plastic zone was first detectable in the optical micrographs at about 3% strain. Although the dark zone ahead of the craze tip in the optical micrographs was thought to be caused by the plastic

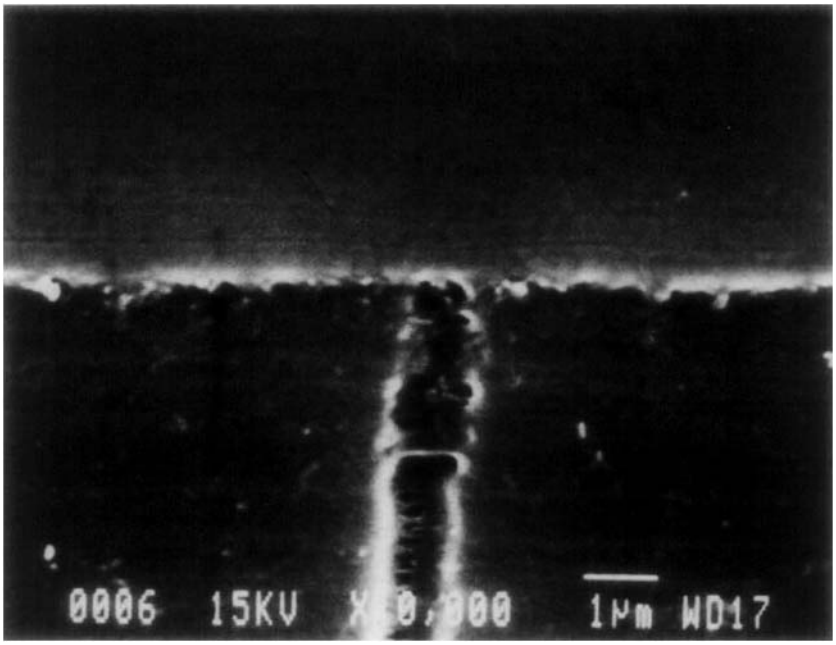

Figure 5 An SEM view of the blunted craze tip at 5.5% strain.

zone, its measured length probably did not accurately represent the dimension of the plastic zone. At 4.5% strain, the craze opening was large enough that fibrils near the surface began to fracture, and micro-shearbands were first visible growing out from the craze tip at an angle of approximately 45°. The micro-shearbands rapidly grew into the PC layer with increasing remote strain; the local strain in the

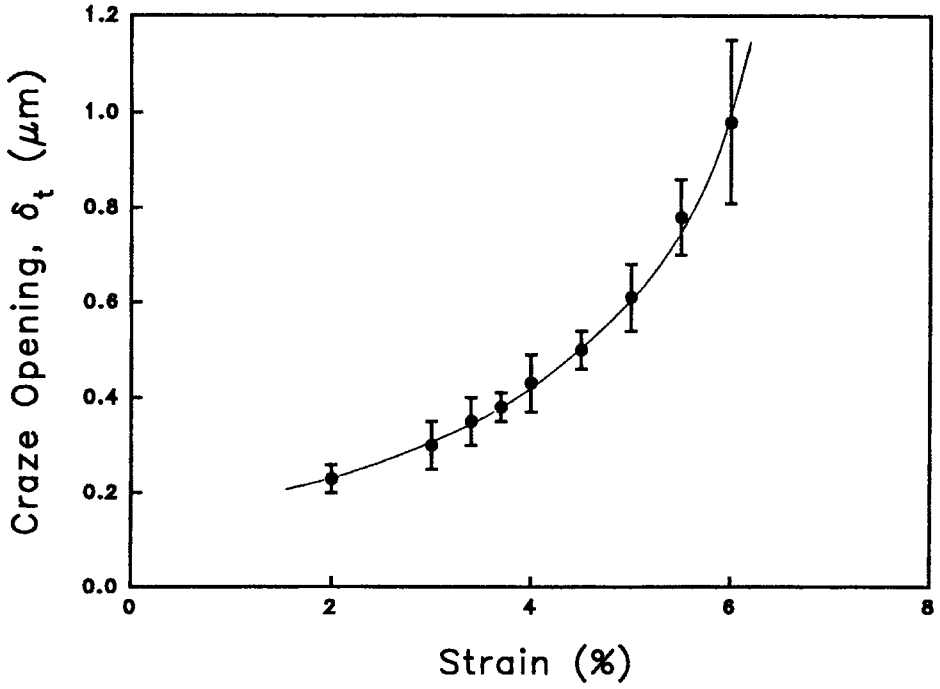

Figure 6 The craze-tip opening determined from scanning electron micrographs as a function of the remote strain.

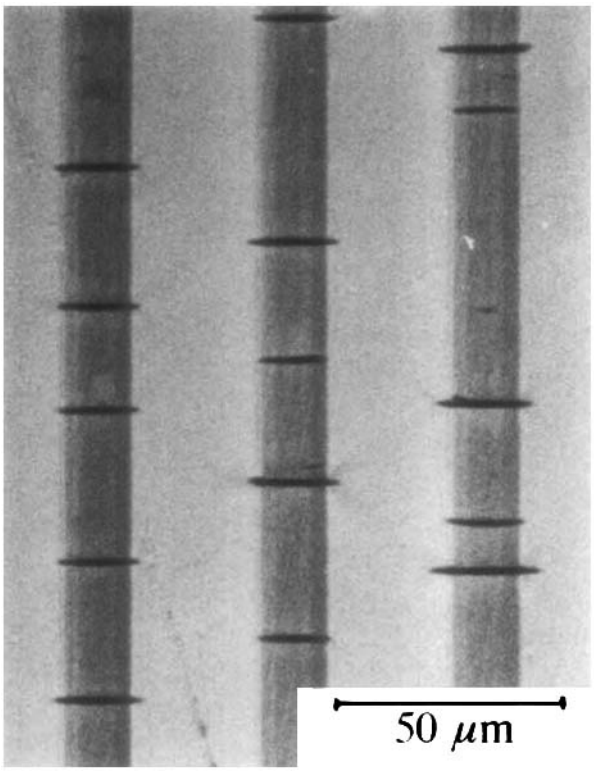

Figure 7 An optical micrograph of crazes at 5.5% strain showing the craze-tip deformation zone in the PC layer.

micro-shearbands was sufficient to cause significant distortion of the interface. When the remote strain reached about 6.2%, global necking was accompanied by drawing of the PC layers while the crazes opened up into large holes that were eventually the site of crack initiation.

Analysis of the Craze-tip Plastic Zone

The deformation zone produced by shear yielding in notched PC has been described for conditions that range from mostly plane strain to mostly plane stress. The primary features of shear yielding in PC, including thickness effects, can be described in terms of idealized elastic–plastic behavior without reference to size scale.[7] It may therefore be possible to apply the prior analysis to a size scale several orders of magnitude smaller to describe the deformation zone that forms in the PC layer at the tip of a SAN craze.

Plane strain shear yielding of PC at a semicircular notch occurs first by core yielding when two families of intersecting flow lines grow out from the notch surface. When further growth of the core yielding zone is constrained by the surrounding elastic material, hinge shear initiates from the surface where a larger degree of freedom is available for extended yielding. The hinge shear bands grow outward from the notch above and below the core yielding zone at an angle of approximately 45°.[7]

Applicability of models for macroscopic yielding behavior to the microdeformation processes in the PC/SAN microlayer composites has been discussed previously. In this regard, the craze tip was viewed as a semicircular micro-notch in the adjacent PC layer, and the deformation was described using a plane strain analogy since the dimension of the craze tip notch, on the order of a micron, was much smaller than the depth of the craze, about 30–50 μm. It was first proposed[2] and then demonstrated[8] that growth of the micro-shearbands at the craze tip with increasing stress follows the same relationship as the growth of the plane strain hinge shear mode in PC.[7] The previous work did not consider the plastic zone that preceded growth of the micro-shearbands at the craze tip. In the plane strain condition, the craze-tip plastic zone would be analogous to the core yielding zone that formed ahead of hinge shear in the macroscopic situation.

The logarithmic spirals of the core yielding zone are described by the slip-line field theory of Hill[9]:

$$\theta = \pm\ln(r/a) + C \tag{4}$$

where r and θ are the polar coordinates; a, the notch radius; and C, a constant. The relationship between the plastic zone length (L_p) and the notch root radius (a) is given by[10]

$$L_p = a[\exp(\pi/2 - \omega/2) - 1] \tag{5}$$

where ω is the flank angle of the notch. For a parallel-sided notch with a circular root (U-notch) or a semicircular notch, $\omega = 0$ and $a = \delta_t/2$, where δ_t is the notch opening, and eq. (5) becomes

$$L_p = 1.9\delta_t \tag{6}$$

This relationship also describes the plastic zone that forms during progressive blunting of a sharp notch in the case of large-scale yielding.[11] A modification of eq. (4) has been proposed to take the pressure dependency of yielding into consideration[12]:

$$\psi \cot\theta = \pm\ln(r/a) + C \tag{7}$$

where 2ψ is the angle between slip lines and is related to the pressure-dependency through $\mu = \cos 2\psi$.[13] For PC, $\mu = 0.07$,[14] and eq. (7) becomes

$$L_p = 2.2\delta_t \tag{8}$$

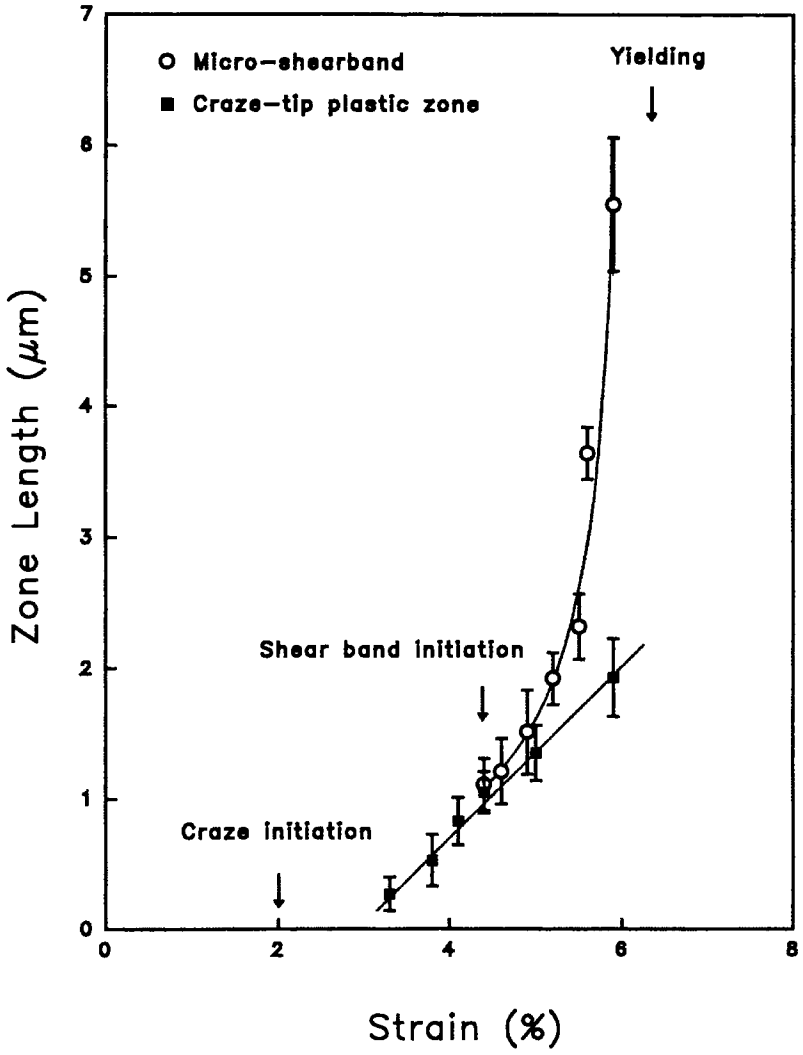

Figure 8 The length of the craze-tip plastic zone and the micro-shearbands as a function of the remote strain.

To apply slip-line theory to analysis of the craze-tip plastic zone, the notch dimension (a) was taken as the radius of curvature of the blunted craze tip determined from scanning electron micrographs. The measured zone length is compared in Table I with that predicted by eq. (8). The magnitude of the plastic-zone length calculated from slip-line theory was consistent with the observations, and the theory also predicted the linear relationship between δ_t and L_p. Measurements of the craze-tip plastic zone taken from optical micrographs were expected to slightly underestimate the length of the plastic zone, especially at the lower strains, since the zone originated from inside the craze tip and was only visible in the optical micrographs when it had grown large enough to produce some surface distortion.

The one-dimensional Dugdale approach has been used to analyze the length of the plastic zone ahead of a notch in thin films.[15] This approach predicts a zone length that is an order of magnitude larger than that calculated with the slip-line theory. Plane stress shear yielding of PC is dominated by the intersecting shear mode, where flow lines extend through the thickness at an angle to produce a necking effect in front of the notch.[7] The plastic zone that forms by intersecting shear at the tip of a blunted sharp notch in thin films of PC is not constrained from growing across the entire specimen width. Qualitatively, the plastic zone formed by plane stress intersecting

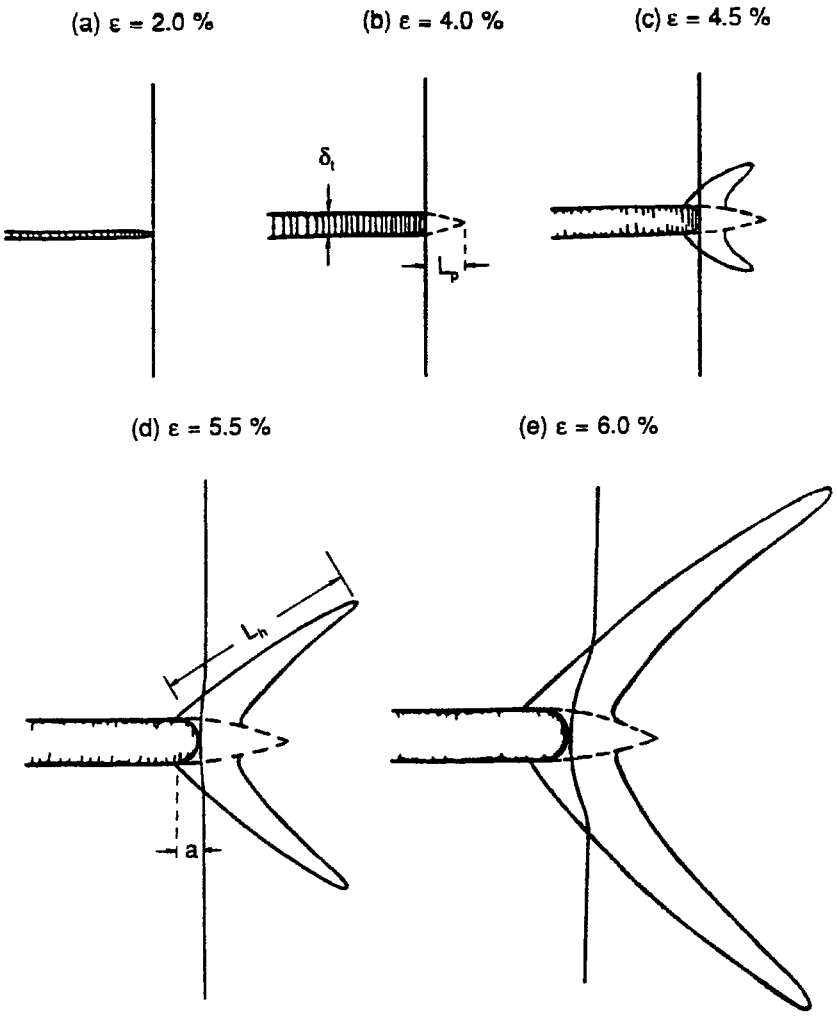

Figure 9 Schematic representation of the formation and growth of the deformation zone in the PC layer at the tip of an SAN craze.

shear is much longer relative to the notch opening than the slip-line zone formed in plane strain loading.

Analysis of the Micro-Shearbands

The approach suggested by Bilby, Cottrell, and Swinden (BCS)[16] has been particularly useful for describing large-scale plane strain yielding by the hinge shear mode although these authors described a plastic zone that was coplanar with the notch. Their result for a notch loaded in shear is similar to Dugdale's relationship for the tensile problem. As noted previously, the Dugdale approach has been used to describe the coplanar plastic zone that forms in thin films of PC loaded in plane stress. It seems reasonable for similar approaches to describe both plane stress and plane strain shear yielding since both BCS and Dugdale employ a one-dimensional approach to obtain a relationship between the notch length and the length of the plastic zone. The hinge shear mode initiates when the shear yield stress is reached at the surface, and like the plane stress intersecting shear mode, hinge shear is not constrained from growing across the entire specimen width. The primary difference is that yielding occurs by different shear modes in plane stress and plane strain shear. As a result, the plastic zone is coplanar in the former case, whereas in the latter case, the plastic zone grows at an angle to the notch.

Tetelman[17] and Hahn and Rosenfield[18] separately observed that experimental values of the plastic-

Table I Comparison of the Experimental Plastic-zone Length with the Theoretical Predictions

Strain (%)	Craze Opening[a] (μm)	Plastic-zone Length (μm)	
		Experimental[b]	Slip Line
3.4	0.35 ± 0.05	0.27 ± 0.13	0.77 ± 0.11
3.7	0.38 ± 0.03	0.53 ± 0.20	0.84 ± 0.07
4.0	0.43 ± 0.06	0.83 ± 0.18	0.95 ± 0.13
4.4	0.50 ± 0.04	1.05 ± 0.16	1.10 ± 0.09
5.0	0.61 ± 0.07	1.35 ± 0.21	1.34 ± 0.15
6.0	0.98 ± 0.17	1.93 ± 0.30	2.16 ± 0.37

[a] Measured from SEM micrographs.
[b] Measured from OM micrographs.

zone length were about a factor of 2 lower than the prediction of BCS for a coplanar zone given by

$$L_h/a = sec(\pi\sigma/2\sigma_Y) - 1 \qquad (9)$$

where L_h is the shear band length; a, the notch radius; and σ_Y, the yield stress. The BCS approach has been extended to yielding on planes inclined to the notch by Bilby and Swinden,[19] who made some limited calculations, and by Vitek.[20] Mills and Walker[21] found that the length of shear bands in the epsilon damage zone of fatigued PC followed the relationship of Vitek for an inclined angle of 65° given by

$$L_h/a = 0.015 \exp[6.642(\sigma/\sigma_Y)] \qquad (10)$$

where L_h is the shear band length; a, the notch radius; and σ_Y, the yield stress.

Ma et al.[7] found that the length of the hinge shear bands that formed at a semicircular edge notch in PC followed the BCS equation [eq. (9)] modified by a factor of 0.5,[17,18] and Ma et al.[2] and Shin et al.[9] observed that the micro-shearbands in PC/SAN composites also followed the modified BCS equation if a constant notch radius of 1 μm was assumed. However, when the crazes were examined at higher magnification by SEM, it was apparent that the craze opening increased as the micro-shearbands lengthened. Present calculations of the zone length made with a notch dimension taken from direct observations of the craze-tip opening necessarily showed a different functional relationship to the normalized stress in the PC layer than did the previous calculations based on a constant notch radius and the remote stress. The stress in the PC layer, σ_{PC}, was calculated according to the rule of mixtures for constant strain, which has the similar form of eq. (2). The yield stress of PC, $\sigma_{Y,PC}$, is about 62.0

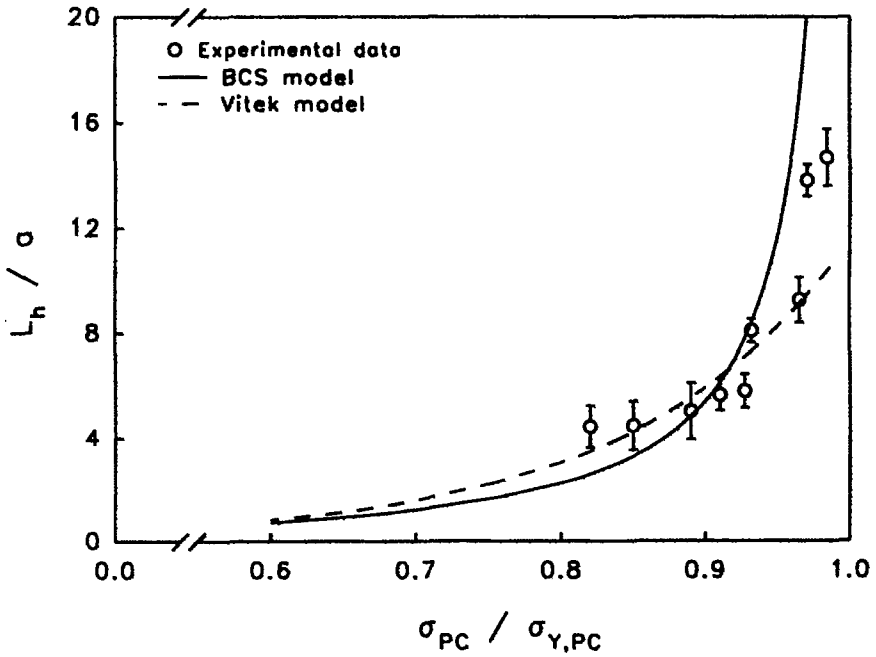

Figure 10 The micro-shearband length compared with predictions of the BCS and Vitek models.

MPa. The ratio L_h/a, determined experimentally from the length of the micro-shearbands and the measured craze opening, is compared with the BCS and Vitek models in Figure 10. Except for the points close to the yield point, the data appear to be described best by the Vitek equation.

CONCLUSIONS

Crazing of SAN and the craze-tip deformation zone that formed in the adjacent PC layer were studied in a microlayer composite with SAN and PC layer thicknesses on the order of tens of microns. Since the PC layer thickness was larger than the deformation zone, it was possible to analyze the deformation zone without considering interactions with neighboring layers. The results led to the following conclusions:

1. The craze density increases with applied stress once the craze initiation condition is achieved in the SAN layers. The relationship between the cumulative craze fraction and the stress on the SAN layers is described by the Weibull distribution function.
2. Crazing occurs randomly in the SAN layers. Statistically, there is no registry or alignment of crazes from one SAN layer to the next.
3. Good adhesion between SAN and PC prevents delamination where the SAN craze impinges on the interface. Instead, a deformation zone forms in the PC layer in response to the stress concentration at the craze tip.
4. The deformation zone can be described by considering two plane strain shear yielding modes on the microscale. Core yielding creates a small colinear plastic zone, whereas the hinge shear mode produces a pair of micro-shearbands that grow away from the craze tip at an angle of about 45°.
5. The length of the plastic zone is accurately predicted by slip-line theory, whereas the length of the micro-shearbands is adequately represented by both the BCS and the Vitek approaches.

The authors wish to thank Dr. J. Im of The Dow Chemical Co. for numerous technical contributions. The generous financial support of the National Science Foundation, Polymers Program (DMR 9100300) is gratefully acknowledged.

REFERENCES

1. B. L. Gregory, A. Siegmann, J. Im, A. Hiltner, and E. Baer, *J. Mater. Sci.*, **22**, 532 (1987).
2. M. Ma, K. Vijayan, J. Im, A. Hiltner, and E. Baer, *J. Mater. Sci.*, **25**, 2039 (1990).
3. D. Haderski, K. Sung, A. Hiltner, and E. Baer, *J. Appl. Polym. Sci.*, **52**, 121 (1994).
4. E. J. Kramer and L. L. Berger, in *Crazing in Polymers*, H. H. Kausch, Ed., Springer-Verlag, New York, 1990, Vol. 2, p. 48.
5. W. Weibull, *J. Appl. Mech.*, **18**, 293 (1951).
6. J. Im, A. Hiltner, and E. Baer, in *High Performance Polymers*, E. Baer and A. Moet, Eds., Hanser, New York, 1991, p. 175.
7. M. Ma, K. Vijayan, A. Hiltner, and E. Baer, *J. Mater. Sci.*, **24**, 2687 (1989).
8. A. Hiltner, K. Sung, E. Shin, S. Bazhenov, J. Im, and E. Baer, *Mater. Res. Soc. Symp. Proc.*, 1992, Vol. 255, p. 141.
9. R. Hill, *The Mathematical Theory of Plasticity*, Clarendon, Oxford, 1950, p. 245.
10. A. S. Tetelman and A. J. McEvily, *Fracture of Structural Materials*, Wiley, New York, 1967, p. 293.
11. J. R. Rice and M. A. Johnson, in *Inelastic Behavior of Solids*, M. F. Kanninen, W. F. Adler, A. R. Rosenfield, and R. I. Jaffee, Eds., McGraw-Hill, New York, 1969, p. 641.
12. J. Salencon, *Application of the Theory of Plasticity in Soil Mechanics*, Wiley, New York, 1977.
13. I. Narisawa, M. Ishikawa, and H. Ogawa, *J. Mater. Sci.*, **15**, 2059 (1980).
14. C. Cheng, P. R. Soskey, S. G. Mylonakis, A. Hiltner, and E. Baer, *J. Appl. Polym. Sci.*, **52**, 177 (1994).
15. I. Narisawa, M. Ishikawa, and H. Ogawa, *Polym. J.*, **8**, 181 (1976).
16. B. A. Bilby, A. H. Cottrell, and K. H. Swinden, *Proc. R. Soc. A*, **272**, 304 (1963).
17. A. S. Tetelman, *ACTA Metall.*, **12**, 993 (1964).
18. G. T. Hahn and A. R. Rosenfield, *ACTA Metall.*, **13**, 293 (1965).
19. B. A. Bilby and K. H. Swinden, *Proc. R. Soc. A*, **285**, 22 (1965).
20. V. Vitek, *J. Mech. Phys. Solids*, **24**, 263 (1976).
21. N. J. Mills and N. Walker, *J. Mater. Sci.*, **15**, 1832 (1980).

Received June 21, 1993
Accepted August 8, 1993